



Sharif University of Technology  
**Scientia Iranica**  
*Transactions A: Civil Engineering*  
<http://scientiairanica.sharif.edu>



# Nonlinearity detection using new signal analysis methods for global health monitoring

Y. Nouri, H. Shariatmadar\*, and F. Shahabian

*Department of Civil Engineering, Faculty of Engineering, Ferdowsi University of Mashhad, Mashhad, P.O. Box 91775-1111, Iran.*

Received 27 April 2021; received in revised form 14 May 2022; accepted 18 October 2022

## KEYWORDS

Structural health monitoring;  
Nonlinearity detection;  
Exploratory data analysis;  
Signal analysis;  
Cross correlation;  
Convolution.

**Abstract.** Statistical pattern recognition has emerged as a promising and practical technique for data-based health monitoring of civil structures. This paper intends to detect nonlinearity changes resulting from damage by some simple but effective signal analysis methods. The primary idea behind these methods is to use measured time-domain vibration signals based on exploratory data analysis without applying any feature extraction. First, statistical moments and central tendency measurements on the basis of the theory of exploratory data analysis are considered as damage indicators to monitor their changes and detect any substantial variations in measured vibration signals. Subsequently, cross correlation and convolution methods are proposed to measure the similarity and overlap between the measured signals of the undamaged and damaged conditions. The main innovation of this study is the capability of the proposed signal analysis methods for implementing nonlinear damage detection without any feature extraction. Numerical and experimental models of civil structures are employed to demonstrate the effectiveness and performance of the proposed methods. Results show that nonlinearity changes caused by damage lead to reductions in the values of cross correlation and convolution methods. Moreover, some statistical criteria are applicable tools for the global structural health monitoring.

© 2023 Sharif University of Technology. All rights reserved.

## 1. Introduction

Structural Health Monitoring (SHM) is a practical process that aims to evaluate the health of civil, mechanical, and aerospace structures. The new branch of this process is carried out by vibration data as a non-destructive strategy for performing damage detection problems [1,2], finite element model updating [3–6], automated operational modal identification [7,8], and

structural life prediction [9]. In the field of SHM, structural damage leads to adverse changes in inherent characteristics of the structure such as mass, stiffness, and damping. These undesirable changes will adversely alter dynamic features or vibration responses. Another effect of damage is the nonlinear behavior that results from stiffness reduction, material failure, and geometric deterioration [10,11].

The process of damage detection can be categorized into the three main levels: (1) damage existence, (2) damage localization, and (3) damage quantification [12]. The primary purpose of the first level is to evaluate whether damage is available throughout the structure [13–17]. This level is usually known as the global health monitoring. The other levels are local

\*. Corresponding author. Tel.: +98 51-38780707;  
Fax: +98 51-38763301  
E-mail address: shariatmadar@um.ac.ir (H. Shariatmadar)

procedures for identifying the damaged area of the structure and estimating the severity of the damage by data-based [18–22] and model-based methods [23–25]. Statistical pattern recognition is a new data-based approach in the process of SHM, which employs signal processing and statistical methods. The implementation of this approach can be divided into four main steps of the operational evaluation, sensing and data acquisition [26], feature extraction, and statistical feature analysis and classification [27].

Feature extraction is a tool for discovering meaningful information, called damage-sensitive features in the field of SHM, from raw measured signals by advanced signal processing methods [28,29]. Among all techniques, one can mention time series analysis [30–33] and operational modal identification [7,8]. Feature analysis/classification exploits the extracted features in an effort to perform the SHM task through machine learning algorithms [34]. Most of the feature classification methods are based on the concept unsupervised learning. This category of machine learning does not need any information (features) of the damaged state of the structure for generating training data [14,35]. In contrast, the other category is supervised learning, which requires information of both undamaged and damaged conditions [36,37]. Generally, the procedures of damage existence and localization can be carried out in an unsupervised learning mode, while the process of damage severity estimation relies on a supervised learning mode [27]. On the other hand, machine learning algorithms are highly useful for the problem of missing data, which is an important challenge in SHM [38].

The key merit of using signal analysis methods is their capability to avoid the feature extraction procedure. Kopsaftopoulos and Fassois [39] used statistical hypothesis testing problems on the basis of nonparametric and parametric methods in order to identify structural damage. The primary idea of their research is that a null hypothesis of the nonparametric or parametric methods is indicative of a healthy condition and an alternative hypothesis implies the damaged condition. Yang et al. [40] proposed a data-based damage detection method by Inner Product Vector (IPV) approach. This method was composed of the cross-correlation of displacements related to the mode shapes extracted from vibration time-domain responses. Wang et al [41] applied the IPV method, which used the cross correlation function of velocity and acceleration time-domain responses. Catbas et al [42] used a correlation-based methodology as an effective nonparametric data analysis approach to detecting and localizing structural changes using strain data. They applied the correlation coefficients of the strain measurements and established a discrepancy matrix by computing the difference of correlation

coefficients between the undamaged and damaged conditions. Sarmadi et al [43] proposed a non-parametric signal processing method based on Ensemble Empirical Mode Decomposition (EEMD) and the well-known Mahalanobis distance for damage localization. Vazirizade et al [44] developed a nonlinear damage detection using the EEMD and artificial neural network.

Despite numerous methods regarding statistical pattern recognition, the process of extracting the damage-sensitive features may be complex, time-consuming, and laborious. In general, it may not be necessary to always extract such features for evaluating the global condition of the structure or finding whether the structure suffers from damage. To tackle this problem, it is feasible to directly analyze raw measured vibration signals without any feature extraction. Accordingly, this article intends to introduce some simple but effective signal analysis methods for the problem of global SHM. The idea behind these methods is to use raw random vibration data by statistical and signal analysis tools. First, some efficient exploratory data analysis measures including statistical moments (i.e., mean, standard deviation, skewness, and kurtosis) and central tendency measurements (median and trimmed mean) are considered as damage and nonlinearity indicators to monitor their variations caused by the occurrence of damage. Second, two non-parametric signal processing techniques based on cross correlation and convolution are suggested to measure the similarity and overlap between vibration time-domain signals in the undamaged and damaged conditions. A new strategy is also developed to use the proposed signal analysis methods for assessing the global SHM. Despite the applications of the statistical moments in signal processing regarding the problem of SHM, the contributions of this research can be summarized as suggesting the central tendency measures and signal analysis methods, particularly based on the signal convolution. Numerical and experimental benchmark structures are applied to verify the accuracy and capability of the proposed methods. Results demonstrate that the cross correlation and convolution methods are potentially able to detect the nonlinearity conditions due to damage occurrence. Moreover, most of statistical criteria, with the exception of mean and standard deviation, properly detect the global state of models.

The layout of this paper is as follows. Section 2 gives fundamental concepts of the exploratory data analysis including discussion about statistical moments and measures of central tendency. In Section 3, the cross correlation and convolution methods are described. Section 4 presents a new strategy for implementing the global SHM. In the following, Sections 5 and 6 demonstrate the accuracy and performance of the proposed methods using a numerical benchmark model of concrete beam and a numerical model of laboratory

frame. Eventually, the conclusions of this study are remarked in Section 7.

## 2. Exploratory data analysis

### 2.1. Statistical moments

In statistics, the statistical moments are important and useful tools for estimating the meaningful information from any kinds of data, particularly for randomly distributed data. The most well-known statistical moments are the mean, standard deviation, variance, skewness, and kurtosis, which can reduce dimensionality of the randomly sampled data and provide a feature of the unit dimension. For a  $k$ -dimensional random data,  $\mathbf{A} = [a_1, a_2, \dots, a_k] \in \mathbb{R}^k$ , the mean ( $\mu$ ) and standard deviation ( $\sigma$ ) are formulated as:

$$\mu = \frac{1}{k} \sum_{i=1}^k \mathbf{A}_i, \tag{1}$$

$$\sigma = \sqrt{\frac{1}{k} \sum_{i=1}^k (\mathbf{A}_i - \mu)^2}. \tag{2}$$

The skewness is a measure of the asymmetry of the probability distribution of a random variable around the sample mean. If skewness is negative, the data are spread out more to the left of the mean than to the right. In contrast, if it is positive, the data are spread out more to the right. The skewness of a random variable with the normal distribution is zero. The skewness ( $\gamma$ ) of a  $k$ -dimensional random data,  $\mathbf{A} \in \mathbb{R}^k$ , is defined as:

$$\gamma = \frac{\frac{1}{k} \sum_{i=1}^k (\mathbf{A}_i - \mu)^3}{\sigma^3}. \tag{3}$$

The kurtosis is a measure of the stretch of the probability distribution of a random variable. In a similar way to the concept of skewness, it is a descriptor of the shape of a probability distribution. In other words, the kurtosis of a probability distribution shows its form based on the kind of data distribution. In this regard, the kurtosis of any univariate normal distribution is 3. The equation of this statistical moment for the random variable,  $\mathbf{A}$ , is given by:

$$\kappa = \frac{\frac{1}{k} \sum_{i=1}^k (\mathbf{A}_i - \mu)^4}{\sigma^4}. \tag{4}$$

The basic idea behind the proposed application of the statistical moments is that nonlinear changes in a structure lead to alterations in the normality of distribution of the measured vibration signals. In most cases, it is an accurate assumption that the vibration response of a healthy structure has a normal distribution; hence, damage alters the normality of

measured vibration data. Therefore, the aforementioned statistical moments are considered to detect nonlinear conditions.

### 2.2. Measures of central tendency

The median and trimmed mean are two measures that are resistant to outliers or abnormal conditions. The sample mean ( $\mu$ ) is sensitive to these problems so that an undesirable data value can move the average away from the center of the rest of the data by an arbitrarily large distance. The median of a finite list of numbers can be found by arranging all the observations from the lowest value to the highest value and picking the middle one. If there is an even number of observations, then there is no single middle value; the median is usually defined to be the mean of the two middle values. The basic idea of the trimmed mean is to ignore a small percentage of the highest and lowest values of a sample when determining the center of the sample. If there are outliers in the data, the trimmed mean is a more representative estimate of the center of the body of the data than the mean. To compute the trimmed mean of a data set (vector)  $\mathbf{A} \in \mathbb{R}^k$ , reorder it from the smallest to the largest value. By choosing a specific percentage, the trimmed mean is calculated as follows:

$$tm = \frac{1}{k-h} \sum_{i=h+1}^{k-h} a_{k:i}, \tag{5}$$

where  $h = k \times p$  and  $p$  is a scalar value denoting the percentage of the removed components from the set  $\mathbf{A}$ . For example, if  $\mathbf{A}$  is a vector with 200 elements ( $k$ ) and  $p = 10\%$ , the scalar value  $h$  is equal to 20. Moreover,  $a_{k:i}$  is the ordered sample of  $\mathbf{A}$ , where  $a_{k:k}$  and  $a_{k:1}$  stand for the maximum and minimum values, respectively. It is worth remarking that the median is the mean trimmed 100% and the arithmetic mean is the mean trimmed 0%.

## 3. Signal analysis methods

### 3.1. Cross correlation

In signal processing, the cross-correlation is a measure of similarity of two series as a function of the lag of one relative to the other. In other words, this method computes the correlation between the two random variables  $\mathbf{X}$  and  $\mathbf{Y}$ . The cross-correlation method places against autocorrelation and partial autocorrelation functions that measure the correlation of a random variable with itself. For the two random distribution data,  $\mathbf{X} \in \mathbb{R}^n$  and  $\mathbf{Y} \in \mathbb{R}^n$ , the vector of cross correlation at delay  $\tau$  is defined as follows:

$$\mathbf{r} = \frac{\sum_{i=1}^n (\mathbf{X}(i) - \mu_X) (\mathbf{Y}(i - \tau) - \mu_Y)}{\sqrt{\sum_{i=1}^n (\mathbf{X}(i) - \mu_X)^2} \sqrt{\sum_{i=1}^n (\mathbf{Y}(i) - \mu_Y)^2}}, \tag{6}$$

where  $\mu_X$  and  $\mu_Y$  denote the mean of random variables  $\mathbf{X}$  and  $\mathbf{Y}$ , respectively. From the signal processing sense, if these random variables are independent data, the probability density of the difference  $\mathbf{Y}-\mathbf{X}$  is formally given by the cross-correlation; however, this terminology is not used in the probability and statistics.

In the context of SHM using the statistical pattern recognition paradigm, the variable  $\mathbf{X}$  denotes a training data set coming from the measured response data in the undamaged and damaged conditions. In addition, the variable  $\mathbf{Y}$  is a test data set that consists of the measured response data in both of the undamaged and damaged conditions. When the test data includes the undamaged vibration signals, the cross correlation computes the correlation of signals between undamaged conditions, which can be chosen as a threshold level. From the correlation theory, any deviation from this level is an indication of nonlinearity changes or damage occurrence.

### 3.2. Convolution

In the signal processing community, the convolution of two signals,  $\mathbf{X}$  and  $\mathbf{Y}$ , represents the area of overlap under the points as  $\mathbf{X}$  slides across  $\mathbf{Y}$  [45]. From a mathematical viewpoint, the convolution is a mathematical operation on two functions, producing a third function that is typically viewed as a modified version of one of the original functions. In the time-domain signals, the convolution of two signals involves integrating (for the continuous signals) and summing (for the discrete signals) the product of the two signals, where one of them is shifted [46]. The equation of convolution for the two random distribution data  $\mathbf{X} \in \mathbb{R}^n$  and  $\mathbf{Y} \in \mathbb{R}^m$  is written in the following form:

$$\mathbf{c} = \sum_{j=-\infty}^{\infty} \mathbf{X}(j) \cdot \mathbf{Y}(q-j+1). \quad (7)$$

In this expression,  $\mathbf{c}$  is the vector of convolution with the length of  $q$ , where  $q = n + m - 1$ . Mathematically, the convolution is similar to the cross-correlation; however, there is a difference between them. In general, the cross correlation is a process to find the degree of similarity between two signals, whereas the convolution is a measure of effect of one signal on the other. In the signal processing, the convolution is a filtering operation and the cross correlation is a measure of relation between two signals.

From the convolution theory, if the structure does not suffer from damage, this indicates that there is an entire overlap between the two measured vibration signals. For a damaged structure, on the other hand, the overlap between the measured vibration data in the two conditions (the undamaged and current) decreases, implying nonlinear changes resulting from damage. In a similar way to the cross-correlation method, the

variables (signals)  $\mathbf{X}$  and  $\mathbf{Y}$  are chosen as the training and test data sets.

### 4. SHM strategy

In order to optimally apply statistical and signal analysis methods in the context of SHM, it is very important to establish a meaningful and applicable framework that facilitates evaluating the state of the structure and detecting any probable damage. In other words, this framework enables us to observe and monitor the structural conditions and use statistical methods. On the basis of the proposed methods in the previous sections, signals in different structural states are compared together to make a decision about the condition of the structure and implement practical global health monitoring.

The easiest approach is to separately compare the sensor signals at the same location in the undamaged and damaged conditions. However, this is a time-consuming and difficult process because it is necessary to compare a large number of sensor signals with numerous cross-correlation or convolution data. To overcome this problem, a new strategy is presented here by collecting measured response data in each structural condition in a vector. Assume that  $\mathbf{X}^*$  and  $\mathbf{Y}^*$  are  $m$ -by- $n$  matrices, where  $m$  is the data samples and  $n$  denotes the number of variables (sensors) in the undamaged and current (possibly damaged) conditions, respectively. As a sample, the undamaged data set (sensor signals) can be expressed as follows:

$$\mathbf{X}^* = \begin{bmatrix} x_{11} & x_{12} & \cdots & x_{1n} \\ x_{21} & \ddots & & x_{2n} \\ \vdots & & \ddots & \vdots \\ x_{m1} & x_{m2} & \cdots & x_{mn} \end{bmatrix}. \quad (8)$$

It is possible to make a vector using a vectorization of this matrix. In mathematics, the matrix vectorization is a linear transformation that converts the matrix into a column vector [3]. For example, the vectorization of the matrix  $\mathbf{X}^*$  is a column vector with  $mn$  elements, where the first  $m$  rows indicate the first column of this matrix. Under such circumstances, the column vectors in the undamaged and damaged conditions are written as follows:

$$\mathbf{X} = [x_{11} \ \dots \ x_{m1} \ x_{12} \ \dots \ x_{m2} \ \dots \ x_{1n} \ \dots \ x_{mn}]^T, \quad (9)$$

$$\mathbf{Y} = [y_{11} \ \dots \ y_{m1} \ y_{12} \ \dots \ y_{m2} \ \dots \ y_{1n} \ \dots \ y_{mn}]^T. \quad (10)$$

With this strategy, all data samples of all sensors in each structural condition are collected into these vectors and they make the proposed methods possible to practically evaluate the global state of the structure. Accordingly, if the vector-style set  $\mathbf{Y}$  belongs to the

damaged condition, one expects to observe significant changes in the proposed signal processing measures.

### 5. Numerical verification

#### 5.1. A benchmark concrete beam

To verify the performance and effectiveness of the proposed methods, a numerical benchmark model of the reinforced concrete beam is used, as shown in Figure 1. The model is a simply supported beam with length 5 m, height 0.5 m, and width 0.01 m constructed based on the Euler-Bernoulli beam theory. It was assumed that similar damping mechanisms were distributed throughout the beam; hence, Rayleigh damping was applied to establish a full damping matrix. The numerical beam was modeled with 4-node linear 2D elements with reduced integration and the ABAQUS Explicit finite element code was used for the simulations [47].

In the simulation process, it was assumed that 15 sensors were installed at the top and bottom of the beam, which measured acceleration time series responses in the transverse or vertical direction at the top or bottom edges of the beam. A randomly uniform transverse load was applied to the top surface of the beam in order to excite the beam. The load

histories were low-pass filtered below 1000 Hz, resulting in five active dynamic modes of the structure. The measurement period was two seconds with 4001 data points. To simulate structural damage, a single vertical crack was modeled at the location of sensor 8 at the bottom edge. This damage realistically simulated a breathing crack with nonlinear behavior, which is a common damage pattern in many concrete structures. Table 1 shows several damage cases with different severities in the numerical beam.

Unlike Ref. [47], the first two measurements of acceleration responses in the undamaged (Measurements 1-2) and damaged (measurements 11-12) cases are chosen for use in the global health monitoring and signal analysis methods. Therefore, the simulated acceleration response data is composed of a matrix with 8002 data points from fifteen sensors under seven damage scenarios. For example, Figure 2 indicates the acceleration time histories of sensor 8 in cases 1 and 7, respectively.

#### 5.2. Normality distribution tests of the vibration responses

One way to understand the nature of the measured vibration signals is to use hypothesis tests. There

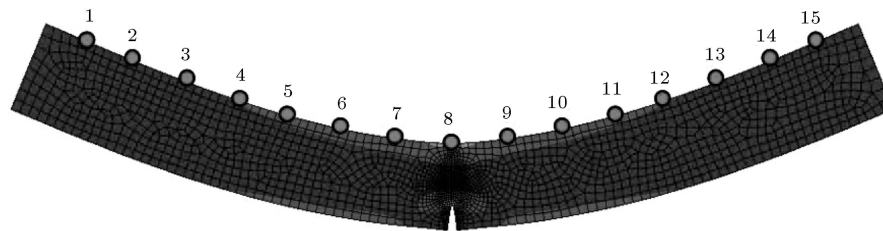


Figure 1. The numerical benchmark concrete beam [47].

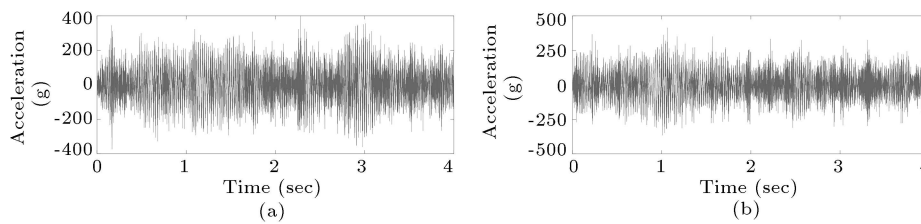


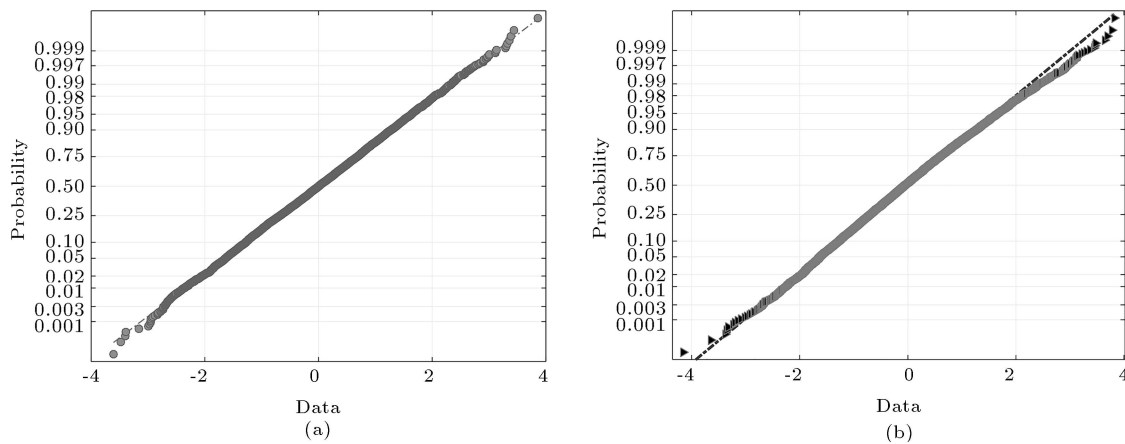
Figure 2. The acceleration time histories at sensor 8 in the numerical beam: (a) Case 1 and (b) case 7.

Table 1. The damage cases in the numerical beam model.

| Case | Structural state | Description           | Performance |
|------|------------------|-----------------------|-------------|
| 1    | Undamaged        | No crack              | Linear      |
| 2    | Damaged          | Crack length = 10 mm  | Nonlinear   |
| 3    | Damaged          | Crack length = 20 mm  | Nonlinear   |
| 4    | Damaged          | Crack length = 30 mm  | Nonlinear   |
| 5    | Damaged          | Crack length = 50 mm  | Nonlinear   |
| 6    | Damaged          | Crack length = 100 mm | Nonlinear   |
| 7    | Damaged          | Crack length = 150 mm | Nonlinear   |

**Table 2.** Hypothesis tests for recognizing the distribution of the measured data.

| Hypothesis tests | Index           | Acceleration response data |                |
|------------------|-----------------|----------------------------|----------------|
|                  |                 | Undamaged                  | Damaged        |
| Chi-square       | <i>p</i> -value | 0.8155                     | 0.0234         |
|                  | Null hypothesis | $\mathbb{H}_0$             | $\mathbb{H}_1$ |
| Anderson-Darling | <i>p</i> -value | 0.5115                     | 0.0005         |
|                  | Null hypothesis | $\mathbb{H}_0$             | $\mathbb{H}_1$ |
| Lilliefors       | <i>p</i> -value | 0.2874                     | 0.0055         |
|                  | Null hypothesis | $\mathbb{H}_0$             | $\mathbb{H}_1$ |



**Figure 3.** The normal plots of acceleration time histories at sensor 8: (a) Case 1 and (b) case 7.

are a large number of tests that can be applied to find the distribution of data. The hypothesis tests are statistical tools that numerically examine the data distributions. All statistical hypothesis tests have the same terminology and structure in such a way that a test may yield a null hypothesis ( $\mathbb{H}_0$ ) or may become an alternative hypothesis ( $\mathbb{H}_1$ ). The former is an assertion about data samples that refers to a general statement in the sense that there is no relationship between the samples and no difference between them. In other words, the null hypothesis means that the test accepts the main assumption under study. On the contrary, the alternative hypothesis is a contrasting assertion about the data that can be tested against the null hypothesis.

Each hypothesis test can present a numeric amount called *p*-value, which is the probability of the test under the null hypothesis. The significance level of a test is a threshold of probability and a typical value of this level is 0.05. If the *p*-value of a test is less than this level, the test rejects the null hypothesis. By contrast, if the *p*-value is greater than the significance level, there is insufficient evidence to reject the null hypothesis. Table 2 shows three hypothesis tests for understanding the normality distribution of the acceleration time

histories at sensor 8 in cases 1 (undamaged) and 7 (damaged).

As can be seen from this table, all hypothesis tests in the undamaged state indicate that the acceleration response is normal since the *p*-values of the tests are larger than 0.05 and the null hypotheses are  $\mathbb{H}_0$ . In addition, these tests confirm that the acceleration time history in the damaged case does not have the normal distribution resulting from the *p*-values less than 0.05 and the rejection of the null hypothesis in each test. Thus, it can be argued that the simulated damage changes the normality of the response data.

Another approach to evaluating the normality of data is to apply a graphical tool such as the normal or Q-Q plot. Figure 3 illustrates the normal plots of the acceleration time histories in cases 1 and 7 at the location of sensor 8. Figure 3(a) belongs to the normal plot of the acceleration time history in the undamaged case. It is seen that there is no dispersion in the samples of the normal plot from the straight line. Figure 3(b) shows the normal plot of acceleration time history in the damaged case. As can be observed, some components of the normal plot do not coincide with the straight line, indicating the presence of the non-

normality distribution in the acceleration time history in the damaged condition.

### 5.3. Nonlinearity detection

A damaged structure typically behaves nonlinearly since damage alters the behavior of the structure from a linear state in its undamaged condition to the damaged one. For a damage identification problem, the structure is typically excited at a low level of excitation, which results in linear and elastic dynamic responses, even in the damaged structure. In this section, the statistical criteria, cross correlation, and convolution methods are employed to detect nonlinearity in the beam. Table 3 represents the mean and standard deviation in all cases of the beam.

It is observed that the mean and standard deviation of the acceleration time histories collected into the vectors  $\mathbf{X}$  and  $\mathbf{Y}$  do not substantially change with the damage occurrence. This means that these statistical moments are not appropriate tools for SHM by raw vibration data. On the other hand, Figure 4 illustrates the box plot of the other statistical criteria including the median, trimmed mean, skewness, and kurtosis for evaluating the global state of the beam.

As shown in Figure 4, all of the statistical criteria change due to the emergence of damage. It is clear that the median, the trimmed mean, and the kurtosis increase by increasing the damage severity from the second case to the seventh case. In addition, the values

of skewness are reduced by increasing the damage extent. In this figure, case 7 has the highest dispersion in comparison with the other damaged cases. Such alterations imply that these criteria are useful for assessing the global state of structures for monitoring their behavior.

In order to detect nonlinear changes in the numerical beam, the matrices of the acceleration time histories of the fifteen sensors regarding the undamaged and damaged conditions are converted into the column vectors based on Eqs. (9) and (10). Subsequently, one only needs to determine the vectors of cross-correlation and convolution. Figure 5 illustrates the results of cross-correlation method in the case of beam in the undamaged or baseline condition (case 1), the damaged state with the lowest level of the damage severity (case 2), and the damaged state with the highest level of the damage severity (case 7). As Figure 5 shows, there are several large and striking peaks in the cross-correlation values of the undamaged condition in comparison with the corresponding cross-correlation values of the damaged states. On this basis, one can consider such peaks as thresholds for nonlinearity detection. Furthermore, the values of cross-correlation decrease by increasing the level of damage from case 1 to cases 2 and 7 so that the state with the highest damage severity (case 7) has the lowest cross-correlation quantities. This means that there is no similarity between the cross-correlation

**Table 3.** The values of mean and standard deviation in the beam.

| Cases | Mean    | Standard deviation |
|-------|---------|--------------------|
| 1     | 0.00039 | 0.9929             |
| 2     | 0.00038 | 1.0677             |
| 3     | 0.00041 | 1.0694             |
| 4     | 0.00042 | 1.0710             |
| 5     | 0.00040 | 1.0727             |
| 6     | 0.00039 | 1.0721             |
| 7     | 0.00043 | 1.0516             |

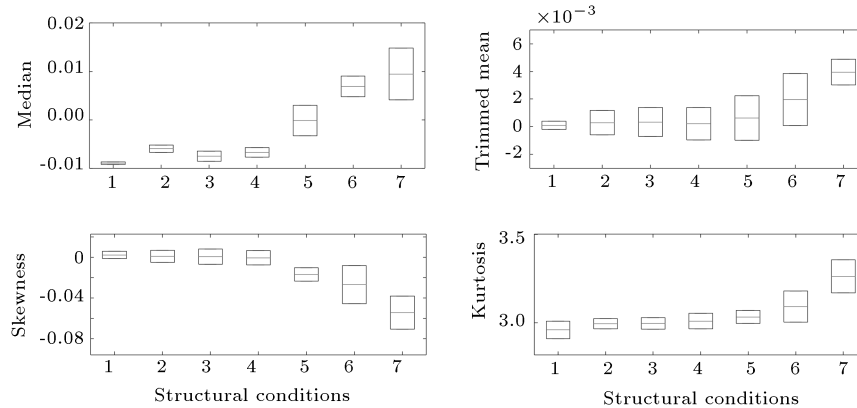


**Figure 4.** The statistical criteria for the global structural health monitoring in the beam.

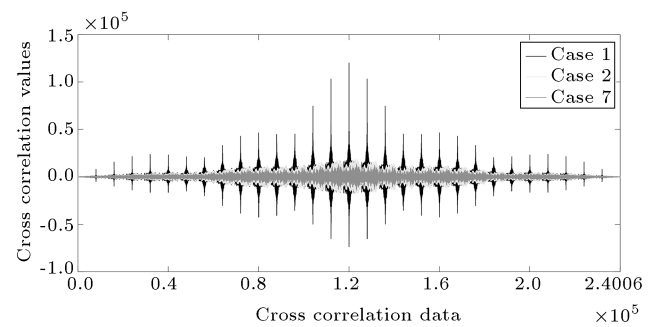


**Figure 5.** Nonlinearity detection by the cross-correlation method in cases 1, 2, and 7.

values of these cases due to the occurrence of damage in the numerical beam. In fact, the elimination of peaks is indicative of the dissimilarity between the vibration signals of the undamaged and damaged conditions. Figure 6 indicates the convolution values of sets **X** and **Y**. As can be seen, the damage to the beam leads to a clear reduction in the convolution values; however, unlike the cross-correlation method, there are not striking peaks in the convolution method.

One way to quantitatively evaluate the global state of the beam is to compute Euclidean norm of cross correlation and convolution vectors. Having considered are the vectors of the cross correlation and convolution **r** and **c**; hence, the Euclidean norms of these vectors are defined as  $e_r = ||\mathbf{r}||_2$  and  $e_c = ||\mathbf{c}||_2$ , respectively. Figure 7 shows the amounts of these norms in cases 1–7. As can be observed, the norms of the cross correlation and convolution in the damaged cases are reduced by increasing the level of the damage. In Figure 7, the largest norm value belongs to the undamaged condition and the damaged case 7 has the smallest quantity. Therefore, it can be concluded that damage leads to the reduction of the norms of the cross correlation and convolution vectors. Although the values of these methods are different, both of them have similar Euclidean norm amounts.

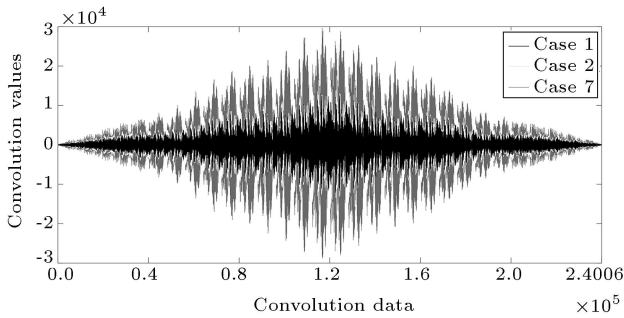


**Figure 6.** Nonlinearity detection by the convolution method in cases 1, 2, and 7.

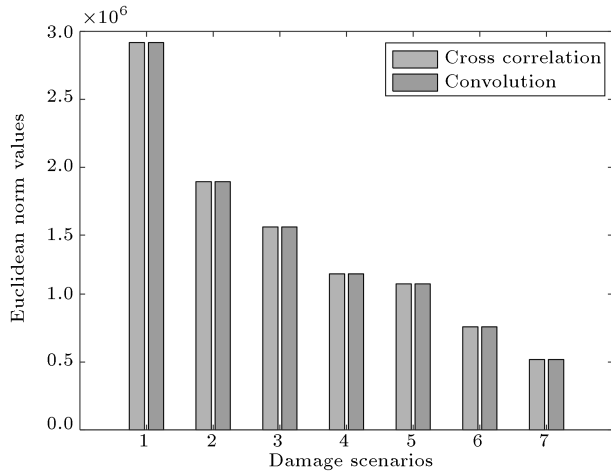


**Figure 7.** Euclidean norms of the cross correlation and convolution methods.

## 6. Experimental validation

### 6.1. A laboratory benchmark model

The validation of the proposed methods for nonlinearity detection is then carried out by a set of experimental data from a laboratory benchmark model with the nonlinear behavior due to damage occurrence. This model is a three-story aluminum frame, as shown in Figure 8. The schematic and sensor locations in the frame are displayed in Figure 9. Four accelerometers were mounted on the floors and a random vibration load was applied by means of an electrodynamic shaker to the base floor along the center line of the frame. The experimental data includes acceleration time histories acquired from the mounted sensors at each floor. The sensor signals were sampled at 320 Hz for 25.6 seconds in duration discretized into 8192 data sampled at 3.125 microsecond intervals. Further details about the test structure are available in [27].

Nonlinear damage was introduced by contracting a suspended column with a bumper mounted on the floor below to simulate fatigue crack that could open and close under loading conditions or loose connections in the structure. Different levels of damage severity were created by diverse gap distances between the suspended column and the bumper. Table 4 shows five damaged conditions as well as an undamaged (baseline) condition of the test structure. The baseline condition represents a healthy state in the frame in the sense that there no linear or nonlinear changes in the test structure. In the damaged conditions, 0.20 mm gap distance implies the lowest level of damage, whereas 0.05 mm gap distance is an indication of the highest one. As a sample, Figures 10 and 11 illustrate the vibration load data (input signals) at channel 1 and the

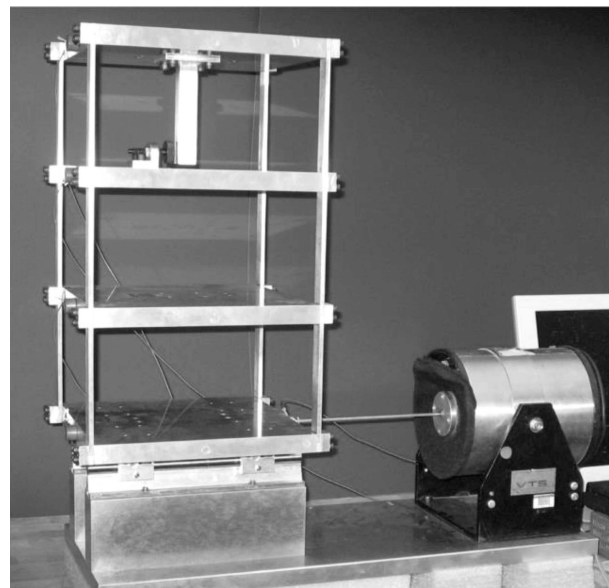


**Figure 8.** The three-story laboratory frame [27].

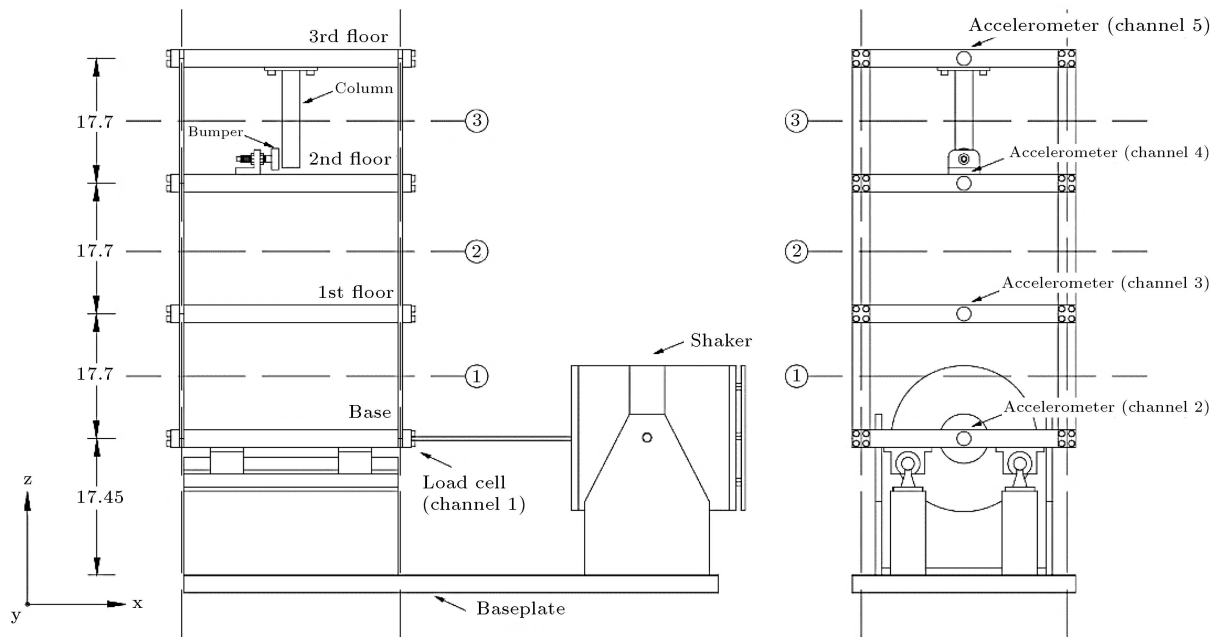


Figure 9. Basic dimensions of the three-story building structure [27].

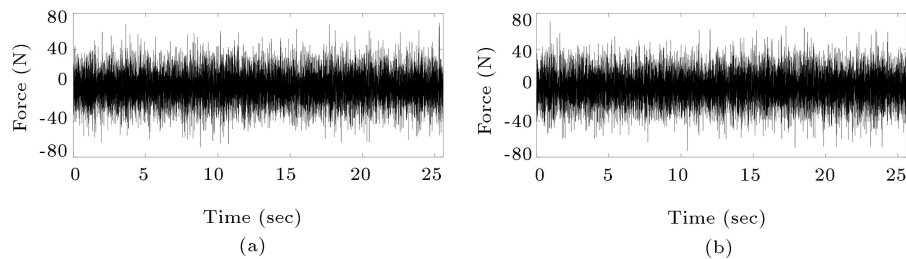


Figure 10. The vibration load signals of the test structure at channel 1: (a) Case 1 and (b) case 6.

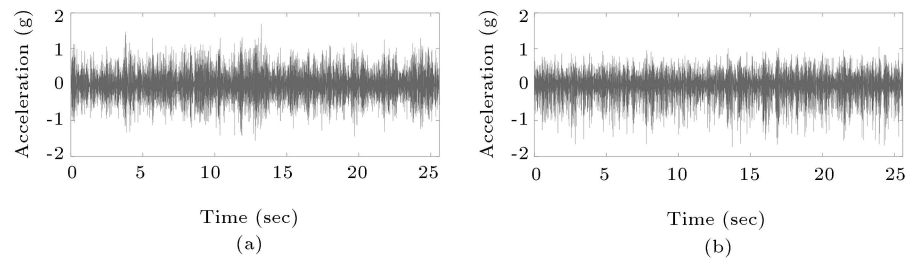


Figure 11. The acceleration response signals of the test structure at channel 5: (a) Case 1 and (b) case 6.

Table 4. The damage scenarios in the laboratory frame [27].

| Case | Condition | Description                                    | Performance |
|------|-----------|--|-------------|
| 1    | Baseline  | Healthy  | Linear      |
| 2    | Damaged   | Distance between bumper and column tip 0.20 mm | Nonlinear   |
| 3    | Damaged   | Distance between bumper and column tip 0.15 mm | Nonlinear   |
| 4    | Damaged   | Distance between bumper and column tip 0.13 mm | Nonlinear   |
| 5    | Damaged   | Distance between bumper and column tip 0.10 mm | Nonlinear   |
| 6    | Damaged   | Distance between bumper and column tip 0.05 mm | Nonlinear   |

acceleration responses (output signals) at the location of channel 5 in cases 1 (baseline condition) and 6 (the highest damage scenario), respectively.

**6.2. Normality distribution tests of the vibration responses**

In order to realize the nature of vibration data, either input (the excitation force) or output signals (the acceleration time histories), the normality distribution tests including chi-square, Anderson-Darling, and Lilliefors are implemented in this section. In this regard, the random vibration load signal subjected to channel 1 and the acceleration time histories acquired at channel 5 in the undamaged (case 1) and damaged (case 6) conditions are examined. Table 5 indicates these hypothesis tests to perceive whether the vibration signals in the laboratory frame in the structural conditions are normal.

From Table 2, it can be understood that the input signals in both healthy and damaged conditions are normal since the amounts of *p*-value in these cases are larger than 0.05 and the results of null hypothesis

are  $\mathbb{H}_0$ . The same conclusions can be achieved for the output signal of the healthy condition; however, the corresponding result in the damaged state shows that there is no normal distribution in the acceleration response of the damaged condition. This observation is valid for the other damaged scenarios.

For further investigation, Figures 12 and 13 display the normal plots of the excitation forces and the acceleration responses, respectively. As shown in Figure 12, both of the excitation signals in the undamaged and damaged conditions have normal distributions. In addition, the normal plot in Figure 13(a) demonstrates a normality distribution for the acceleration signal in the undamaged condition, whereas there is an obvious dispersion in the components of the normal plot in Figure 13(b). This observation suggests that the acceleration time history in the damaged condition does not have normal distribution. As a consequence, the obtained results in this section confirm that the nonlinear change caused by damage alters the normality of random vibration data. However, this conclusion depends on the type of vibration load, that is, if the

**Table 5.** The hypothesis tests for the recognition of data normality distribution.

| Hypothesis tests | Index           | Input signals  |                | Output signals |                |
|------------------|-----------------|----------------|----------------|----------------|----------------|
|                  |                 | Healthy        | Damaged        | Healthy        | Damaged        |
| Chi-square       | <i>p</i> -value | 0.1613         | 0.4668         | 0.5653         | 0              |
|                  | Null hypothesis | $\mathbb{H}_0$ | $\mathbb{H}_0$ | $\mathbb{H}_0$ | $\mathbb{H}_1$ |
| Anderson-Darling | <i>p</i> -value | 0.2748         | 0.1862         | 0.5768         | 0.0005         |
|                  | Null hypothesis | $\mathbb{H}_0$ | $\mathbb{H}_0$ | $\mathbb{H}_0$ | $\mathbb{H}_1$ |
| Lilliefors       | <i>p</i> -value | 0.1545         | 0.2778         | 0.3886         | 0.001          |
|                  | Null hypothesis | $\mathbb{H}_0$ | $\mathbb{H}_0$ | $\mathbb{H}_0$ | $\mathbb{H}_1$ |

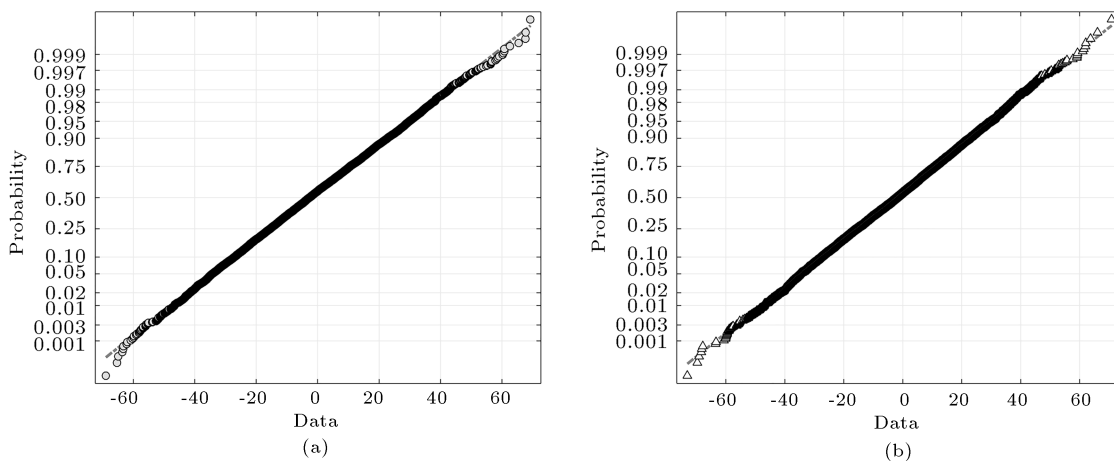


**Figure 12.** The normal plots of the excitation force at channel 1: (a) Case 1 and (b) case 6.

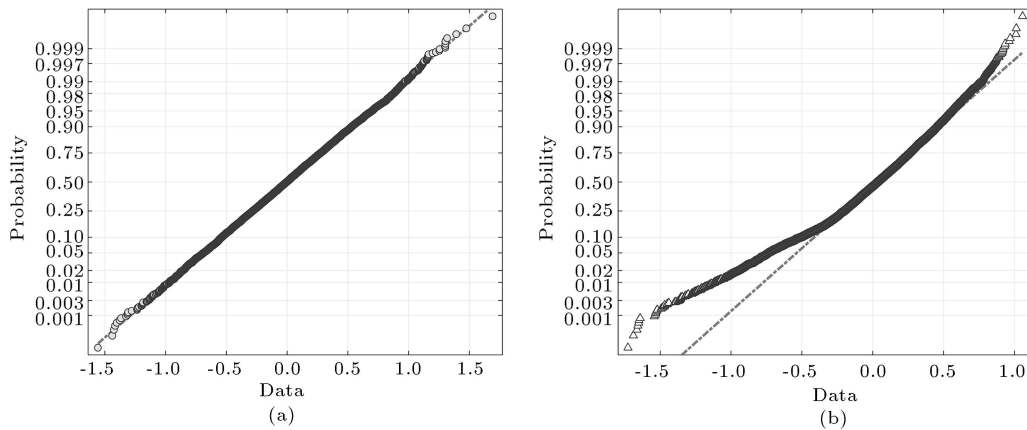


**Figure 13.** The normal plots of the output signals (acceleration time histories) at channel 5: (a) The healthy state and (b) the sixth damaged state.

input signal or the random vibration load applied to an undamaged structure has a normal distribution, the dynamic responses of the structure will be normal.

**6.3. Nonlinearity detection**

In this section, the proposed statistical and signal analysis methods are considered to detect the nonlinear changes in the laboratory frame caused by the occurrence of damage. For this purpose, the matrices of acceleration responses of all sensors in each case are transformed into a column vector; hence, the response data vectors are applied to compute the statistical moments and central tendency measurements. Table 6 indicates the results of mean and standard deviation for the vectors of vibration signals in all structural conditions. Based on the data given in this table, the amounts of the mean and standard deviation are not altered significantly from the second case to the sixth case, meaning that these statistical moments fail to detect the nonlinearity change properly.

Figure 14 shows variations in the median and trimmed mean related to the central tendency measures as well as the skewness and kurtosis. As can be observed in Figure 14, the frame conditions differ such that the values of median, trimmed mean, and kurtosis

**Table 6.** The values of mean and standard deviation of the vectors of response data.

| Cases | Mean    | Standard deviation |
|-------|---------|--------------------|
| 1     | -0.0037 | 0.4755             |
| 2     | -0.0051 | 0.4844             |
| 3     | -0.0038 | 0.4611             |
| 4     | -0.0038 | 0.4652             |
| 5     | -0.0038 | 0.4278             |
| 6     | -0.0037 | 0.3754             |

increase with increasing the level of the nonlinear damage, whereas there is a remarkable reduction in the value of skewness. In this figure, the sixth damage scenario involves the highest dispersion in comparison with the other cases, particularly the undamaged condition. On the other hand, Figures 15 and 16 display the results of cross correlation and convolution methods for detecting changes in the nonlinearity of the laboratory frame, respectively.

From Figure 15, there are several striking peaks at the cross-correlation of the first case. Moreover, the values of cross correlation are reduced by increasing the level of damage. Comparing these values between

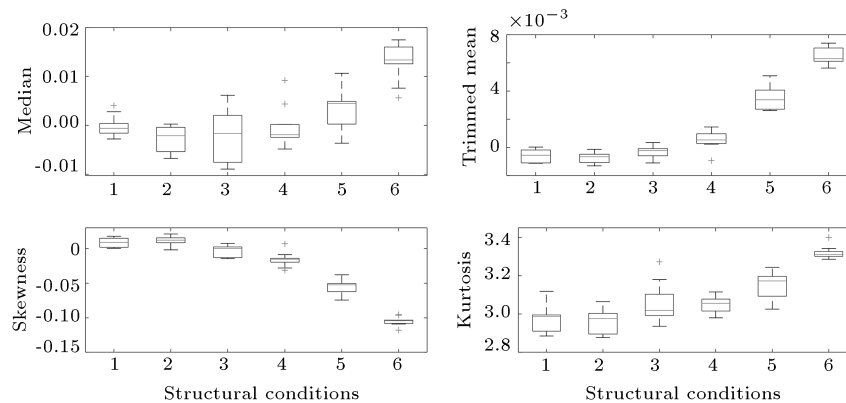


**Figure 14.** The statistical criteria for the global SHM in the frame.

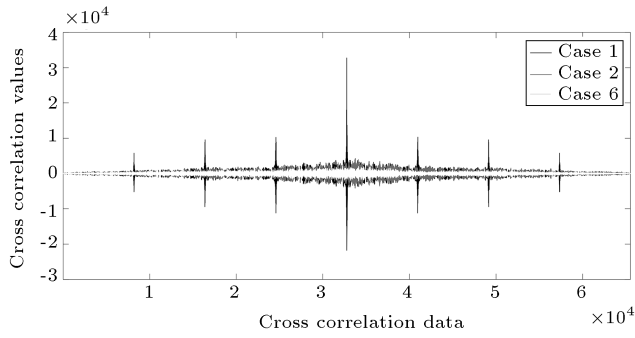


**Figure 15.** Nonlinearity detection in the frame by the cross-correlation method in cases 1, 2, and 6.

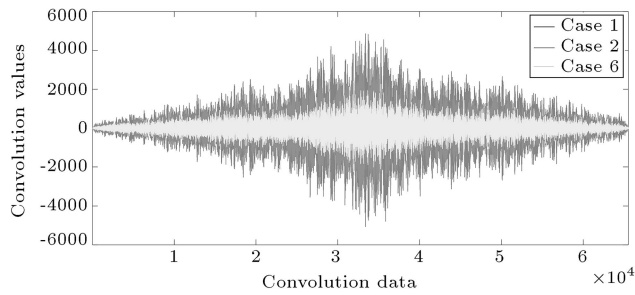


**Figure 16.** Nonlinearity detection in the frame by the convolution method in cases 1, 2, and 6.

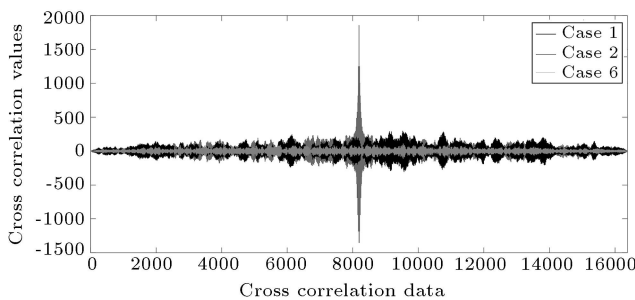


**Figure 17.** Nonlinearity detection by the cross-correlation method at sensor 4 in cases 1, 2, and 6.

the lowest level of damage (case 2) and the highest one (case 6), one can realize that damage leads to a reduction in the cross-correlation values. Figure 16 compares the vectors of convolution values in cases 1, 2, and 6. This figure reveals that there is no similarity among these conditions. Thus, it can be deduced that the damage reduces the values of convolution.

For further investigation, Figures 17 and 18 display the results obtained from cross correlation and convolution methods at the location of channel 4 in cases 1, 2, and 6. The main reason for choosing this sensor is that the location of nonlinear damage (the gap between the bumper and suspended column) in the laboratory frame has been defined at this channel.

From Figure 17, it can be perceived that the cross correlation of channel 4 in the undamaged condition has a large and remarkable peak in comparison with other damaged cases. This means that the vibration

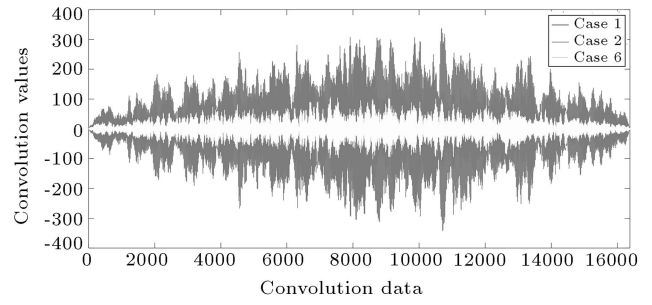


**Figure 18.** Nonlinearity detection by the convolution method at sensor 4 in cases 1, 2, and 6.

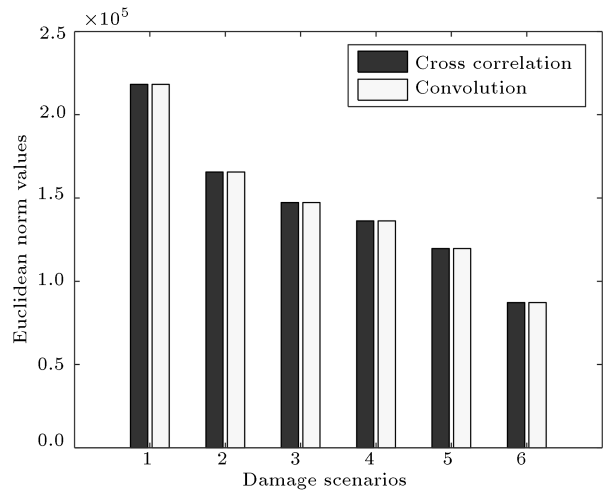


**Figure 19.** The variances of cross correlation and convolution in all cases at sensor #4.

signals at this channel resulting from the damage are not similar in terms of cross correlation. As the large peak is not available in cases 2 and 6, this implies the occurrence of damage or nonlinear conditions.

In contrast to the cross-correlation method, as Figure 18 appears, there is not any striking peak in the convolution of the acceleration response data of the first case. However, it is seen that the quantities of convolution reduce upon increasing the damage severity from cases 1 to 6. Comparing the results obtained from cross-correlation and convolution methods, one can understand that the former outperforms the latter due to the possibility of producing a threshold level (the striking high peak) from the vibration signals in the undamaged condition.

Eventually, Figure 19 shows the Euclidean norms of the cross-correlation and convolution vectors in all scenarios. Accordingly, the Euclidean norms of these methods decrease by increasing the severity of damage. Similar to the numerical model, the result verifies that the damage to the frame leads to serious reductions in the values of cross-correlation and convolution. Another conclusion is concerned with the similarity of the norm values in these methods. Although the cross correlation and convolution experience different levels of variation, they yield the same Euclidean norms.

## 7. Conclusion

This article aimed to introduce new signal analysis methods to detect nonlinear changes due to damage occurrence in civil structures. Initially, the statistical moments including the mean, standard deviation, skewness, and kurtosis as well as the central tendency measurements such as the median and trimmed mean were applied to examine their numerical amounts in different structural conditions. In the following, the cross-correlation and convolution methods were proposed to find the similarity and overlap between the vibration signals in the undamaged and damaged conditions. To use these methods for assessing the global Structural Health Monitoring (SHM), a new strategy was presented through the vectorization of the multivariate datasets of the vibration signals.

On the basis of the numerical and experimental benchmark models, the mean and standard deviation of the acceleration responses failed to detect nonlinear changes, whereas the other statistical criteria could trigger structural changes due to the occurrence of nonlinear damage. As the main conclusion, the values of the median, trimmed mean, and kurtosis increased by increasing the severity of damage, while a contrary result was obtained from the skewness criterion. The normal plots of the acceleration time-domain data showed that if the excitation signals subjected the structure to be normal, damage could change their normality. This conclusion was numerically verified by the chi-square, Darling-Anderson, and Lilliefors hypothesis tests.

Furthermore, nonlinear damage could cause significant reductions in the cross correlation and convolution values. On the other hand, the Euclidean norms of these methods reduced with increasing the level of damage, confirming the capability of cross correlation and convolution methods for detecting nonlinear changes. The comparison of the cross-correlation and convolution methods indicated that the former could provide an obvious threshold level as the striking peaks, making it more practical than the convolution method. This is because such peaks did not observe the convolution values of the vibration signals of the undamaged conditions.

For further research, it is recommended that the proposed methods be evaluated or developed by using different excitation load and noise levels. This is because the excitations of undamaged and damaged conditions may be quite different in forms and energy. In another numerical study, it is suggested that smaller ratios of stiffness reductions be investigated so as to simulate minor damage scenarios.

## Acknowledgement

The authors would like to acknowledge the Engineering

Institute at Los Alamos National Laboratory for accessing the entire experimental data of the three-story laboratory frame. Moreover, we are deeply grateful to Dr. Kullaa for the numerical benchmark model of concrete beam.

## References

1. Qarib, H. and Adeli, H. "Recent advances in health monitoring of civil structures", *Scientia Iranica*, **21**(6), pp. 1733–1742 (2014).
2. Hou, R. and Xia, Y. "Review on the new development of vibration-based damage identification for civil engineering structures: 2010–2019", *Journal of Sound and Vibration*, **491**, 115741 (2021).
3. Sarmadi, H., Karamodin, A., and Entezami, A. "A new iterative model updating technique based on least squares minimal residual method using measured modal data", *Applied Mathematical Modelling*, **40**(23), pp. 10323–10341 (2016).
4. Aditya, G. and Chakraborty, S. "Sensitivity based health monitoring of structures with static response", *Scientia Iranica*, **15**(3), pp. 267–274 (2008).
5. Rezaiee-Pajand, M., Sarmadi, H., and Entezami, A. "A hybrid sensitivity function and Lanczos bidiagonalization-Tikhonov method for structural model updating: Application to a full-scale bridge structure", *Applied Mathematical Modelling*, **89**, pp. 860–884 (2021).
6. Rezaiee-Pajand, M., Entezami, A., and Sarmadi, H. "A sensitivity-based finite element model updating based on unconstrained optimization problem and regularized solution methods", *Structural Control and Health Monitoring*, **27**(5), e2481 (2020).
7. García-Macías, E. and Ubertini, F. "MOVA/MOSS: Two integrated software solutions for comprehensive Structural Health Monitoring of structures", *Mechanical Systems and Signal Processing*, **143**, 106830 (2020).
8. Sedehi, O., Katafygiotis, L.S., and Papadimitriou, C. "Hierarchical Bayesian operational modal analysis: Theory and computations", *Mechanical Systems and Signal Processing*, **140**, 106663 (2020).
9. Saberi, M.R., Rahai, A.R., Sanayei, M., et al. "Steel bridge service life prediction using bootstrap method", *International Journal of Civil Engineering*, **15**, pp. 51–61 (2016).
10. Worden, K., Farrar, C.R., Haywood, J., et al. "A review of nonlinear dynamics applications to structural health monitoring", *Structural Control and Health Monitoring*, **15**(4), pp. 540–567 (2008).
11. Amezcua-Sanchez, J.P. and Adeli, H. "Nonlinear measurements for feature extraction in structural health monitoring", *Scientia Iranica*, **26**(6), pp. 3051–3059 (2019).
12. Gharehbaghi, V.R., Noroozinejad Farsangi, E., Noori, M., et al. "A critical review on structural health

- monitoring: Definitions, methods, and perspectives”, *Archives of Computational Methods in Engineering*, **29**, pp. 2209–2235 (2021).
13. Entezami, A., Shariatmadar, H., and Mariani, S. “Early damage assessment in large-scale structures by innovative statistical pattern recognition methods based on time series modeling and novelty detection”, *Advances in Engineering Software*, **150**, 102923 (2020).
  14. Sarmadi, H. and Yuen, K.-V. “Early damage detection by an innovative unsupervised learning method based on kernel null space and peak-over-threshold”, *Computer-Aided Civil and Infrastructure Engineering*, **36**(9), pp. 1150–1167 (2021).
  15. Entezami, A., Shariatmadar, H., and De Michele, C. “Non-parametric empirical machine learning for short-term and long-term structural health monitoring”, *Structural Health Monitoring*, **21**(6), pp. 2700–2718 (2022).
  16. Daneshvar, M.H. and Sarmadi, H. “Unsupervised learning-based damage assessment of full-scale civil structures under long-term and short-term monitoring”, *Engineering Structures*, **256**, 114059 (2022).
  17. Sarmadi, H. and Yuen, K.-V. “Structural health monitoring by a novel probabilistic machine learning method based on extreme value theory and mixture quantile modeling”, *Mechanical Systems and Signal Processing*, **173**, 109049 (2022).
  18. Entezami, A. and Shariatmadar, H. “Damage localization under ambient excitations and non-stationary vibration signals by a new hybrid algorithm for feature extraction and multivariate distance correlation methods”, *Structural Health Monitoring*, **18**(2), pp. 347–375 (2019).
  19. Entezami, A. and Shariatmadar, H. “Structural health monitoring by a new hybrid feature extraction and dynamic time warping methods under ambient vibration and non-stationary signals”, *Measurement*, **134**, pp. 548–568 (2019).
  20. Feizi, Y.A., Sharbatdar, M.K., Mahjoub, R., et al. “Identifying damage location under statistical pattern recognition by new feature extraction and feature analysis methods”, *Scientia Iranica*, **29**(6), pp. 2789–2802 (2021).
  21. Entezami, A., Shariatmadar, H., and Karamodin, A. “Data-driven damage diagnosis under environmental and operational variability by novel statistical pattern recognition methods”, *Structural Health Monitoring*, **18**(5–6), pp. 1416–1443 (2019).
  22. Dabbagh, H., Ghodrati Amiri, G., and Shaabani, S. “Modal data-based approach to structural damage identification by means of imperialist competitive optimization algorithm”, *Scientia Iranica*, **25**(3), pp. 1070–1082 (2018).
  23. Entezami, A., Shariatmadar, H., and Sarmadi, H. “Structural damage detection by a new iterative regularization method and an improved sensitivity function”, *Journal of Sound and Vibration*, **399**, pp. 285–307 (2017).
  24. Sarmadi, H., Entezami, A., and Ghalehnovi, M. “On model-based damage detection by an enhanced sensitivity function of modal flexibility and LSMR-Tikhonov method under incomplete noisy modal data”, *Engineering with Computers*, **38**(1), pp. 111–127 (2022).
  25. Daneshvar, M.H., Saffarian, M., Jahangir, H., et al. “Damage identification of structural systems by modal strain energy and an optimization-based iterative regularization method”, *Engineering with Computers*, pp. 1–21 (2022).
  26. Amezcuita-Sanchez, J.P., Valtierra-Rodriguez, M., and Adeli, H. “Wireless smart sensors for monitoring the health condition of civil infrastructure”, *Scientia Iranica*, **25**(6), pp. 2913–2925 (2018).
  27. Farrar, C.R. and Worden, K., *Structural Health Monitoring: A Machine Learning Perspective*, Chichester, West Sussex, United Kingdom: John Wiley & Sons Ltd (2013).
  28. Amezcuita-Sanchez, J.P. and Adeli, H. “Signal processing techniques for vibration-based health monitoring of smart structures”, *Archives of Computational Methods in Engineering*, **23**(1), pp. 1–15 (2016).
  29. Zhang, C., Mousavi, A.A., Masri, S.F., et al. “Vibration feature extraction using signal processing techniques for structural health monitoring: A review”, *Mechanical Systems and Signal Processing*, **177**, 109175 (2022).
  30. Entezami, A., Shariatmadar, H., and Karamodin, A. “Improving feature extraction via time series modeling for structural health monitoring based on unsupervised learning methods”, *Scientia Iranica*, **27**(3), pp. 1001–1018 (2020).
  31. Entezami, A. and Shariatmadar, H. “An unsupervised learning approach by novel damage indices in structural health monitoring for damage localization and quantification”, *Structural Health Monitoring*, **17**(2), pp. 325–345 (2018).
  32. Entezami, A., Sarmadi, H., Salar, M., et al. “A novel data-driven method for structural health monitoring under ambient vibration and high dimensional features by robust multidimensional scaling”, *Structural Health Monitoring*, **20**(5), pp. 2758–2777 (2021).
  33. Entezami, A., Sarmadi, H., Behkamal, B., et al. “Big data analytics and structural health monitoring: A statistical pattern recognition-based approach”, *Sensors*, **20**(8), 2328 (2020).
  34. Amezcuita-Sanchez, J. and Adeli, H. “Feature extraction and classification techniques for health monitoring of structures”, *Scientia Iranica., Transaction A, Civil Engineering*, **22**(6), 1931 (2015).
  35. Sarmadi, H. and Karamodin, A. “A novel anomaly detection method based on adaptive Mahalanobis-squared distance and one-class kNN rule for structural health monitoring under environmental effects”, *Mechanical Systems and Signal Processing*, **140**, 106495 (2020).

36. Entezami, A., Shariatmadar, H., and Sarmadi, H. “Condition assessment of civil structures for structural health monitoring using supervised learning classification methods”, *Iranian Journal of Science and Technology Transactions of Civil Engineering*, **44**, pp. 51–66 (2020).
37. Sarmadi, H. and Entezami, A. “Application of supervised learning to validation of damage detection”, *Archive of Applied Mechanics*, **91**(1), pp. 393–410 (2021).
38. Jiang, H., Wan, C., Yang, K., et al. “Continuous missing data imputation with incomplete dataset by generative adversarial networks-based unsupervised learning for long-term bridge health monitoring”, *Structural Health Monitoring*, **21**(3), pp. 1093–1109 (2022).
39. Kopsaftopoulos, F.P. and Fassois, S.D. “Vibration based health monitoring for a lightweight truss structure: Experimental assessment of several statistical time series methods”, *Mechanical Systems and Signal Processing*, **24**(7), pp. 1977–1997 (2010).
40. Yang, Z., Wang, L., Wang, H., et al. “Damage detection in composite structures using vibration response under stochastic excitation”, *Journal of Sound and Vibration*, **325**(4), pp. 755–768 (2009).
41. Wang, L., Yang, Z., and Waters, T. “Structural damage detection using cross correlation functions of vibration response”, *Journal of Sound and Vibration*, **329**(24), pp. 5070–5086 (2010).
42. Catbas, F.N., Gokce, H.B., and Gul, M. “Nonparametric analysis of structural health monitoring data for identification and localization of changes: Concept, lab, and real-life studies”, *Structural Health Monitoring*, pp. 1–14 (2012).
43. Sarmadi, H., Entezami, A., and Daneshvar Khorram, M. “Energy-based damage localization under ambient vibration and non-stationary signals by ensemble empirical mode decomposition and Mahalanobis-squared distance”, *Journal of Vibration and Control*, **26**(11–12), pp. 1012–1027 (2020).
44. Vazirizade, S.M., Bakhshi, A., and Bahar, O. “Online nonlinear structural damage detection using Hilbert Huang transform and artificial neural networks”, *Scientia Iranica*, **26**(3), pp. 1266–1279 (2019).
45. Rader, C.M., *Discrete Convolution via Mersenne Transforms. IEEE Transactions on Computers*, **21**(12), pp. 1269–1273 (1972).
46. Selesnick, I.W. and Burrus, C.S. “Fast convolution and filtering”, CRC Press, 24 pages (1998).
47. Kullaa, J., Santaoja, K., and Eymery, A. “Vibration-based structural health monitoring of a simulated beam with a breathing crack”, in Key Engineering Materials. Trans Tech Publ (2013).

## Biographies

**Younes Nouri** received his MSc degree in Civil Engineering-Structure from Ferdowsi University of Mashhad. His research interests are structural health monitoring, seismic design and analysis of structures and finite element analysis, machine learning, data mining, statistical signal processing, and statistical pattern recognition.

**Hashem Shariatmadar** received his BSc degree in 1989 from Tabriz University, MSc degree in 1993, and PhD degree in 1997 from McGill University in Canada in Structural Engineering. Currently, he is an Associate Professor at Ferdowsi University of Mashhad (FUM). His research studies are about structural control, earthquake engineering, and structural health monitoring and he has authored several papers and publications.

**Farzad Shahabian** is currently a Civil Engineering Professor at the Department of Civil Engineering, Ferdowsi University of Mashhad, Iran. His research interests are reliability, plates and shell structures as well as steel design of structures. He has published several papers in high-impact journals and conference proceedings.